International Information and Engineering Technology Association
Advancing the World of Information and Engineering

Annales de Chimie - Science des Matériaux
Vol. 49, No. 5, October, 2025, pp. 515-522
Journal homepage: http://iieta.org/journals/acsm

# Dry Sliding Wear Characteristics of Sintered Preform Al-$Cr_3C_2$ Metal Matrix Composites

Naga Venkata Srinivas Borra[1*], Veera Venkata Krishna Prasad Davuluri[2], M. Venkata Kiran Kumar[3], Ksbsvs Sastry[1]

[1] Department of Mechanical Engineering, Sri Vasavi Engineering College, Tadepalligudem 534101, India
[2] Department of Mechanical Engineering, R.V.R.&.J.C College of Engineering, Chowdavaram 522019, India
[3] Department of Mechanical Engineering, Sasi Institute of Technology and Engineering, Tadepalligudem 534101, India

Corresponding Author Email: bnvsrinu1@gmail.com



https://doi.org/10.18280/acsm.490507

**Received:** 27 August 2025
**Revised:** 15 October 2025
**Accepted:** 21 October 2025
**Available online:** 31 October 2025

***Keywords:***
*$Cr_3C_2$, composite materials, hardness, mechanical properties of materials, metal matrix composites, metals, wear resistance, powder metallurgy*

**ABSTRACT**

Metal matrix composites (MMCs) have emerged as promising materials in materials science due to their ability to meet stringent criteria such as lightweight properties, superior strength, and wear resistance. Aluminium (Al) is widely favored as a matrix metal, often augmented with ceramic additives like $Cr_3C_2$ to enhance wear resistance. This investigation explores the influence of varying chromium carbide ($Cr_3C_2$) weight percentages (0%, 2%, 4%, and 6%) on the dry sliding wear behavior of aluminum-chromium carbide (Al-$Cr_3C_2$) composites. Using powder metallurgy, composites were fabricated, and mechanical properties, including hardness, were investigated. To assess wear performance, a pin-on-disc wear tester was utilized to measure wear rate and coefficient of friction under various conditions. The test parameters included loads ([20, 30, 40] N), sliding speeds ([1, 1.5, 2] m/s), and sliding distances ([500, 1000, 1500, 2000] m). Results showed improved mechanical properties, especially toughness, in MMCs. Wear rate and coefficient of friction exhibited an inverse relationship with sliding speed but a positive correlation with load. Scanning electron microscopy analyzed wear surfaces. Findings indicated Al composites' superior strength and lower wear susceptibility compared to metallic counterparts, with practical implications for longevity in dry sliding conditions. This study underscores the efficacy of MMCs in enhancing material properties, blending the study of composite materials like $Cr_3C_2$ with metals in mechanical property research.

## 1. INTRODUCTION

Aluminium is extensively employed because of its diverse range of physical, chemical, and mechanical characteristics.

Chromium carbide ($Cr_3C_2$) has better high-temperature oxidation resistance due to the formation of a protective $Cr_3C_2$ layer, unlike Sic and $Al_2O_3$ which degrade or crack under thermal shock. It also offers a good balance of hardness and toughness, making it less brittle than Sic and $Al_2O_3$. $Cr_3C_2$ bonds well with metal binders like NiCr, giving superior adhesion and wear resistance in coatings, especially at elevated temperatures.

By integrating numerous ceramic particles into an aluminium matrix, its properties undergo alteration, thus facilitating its utilization across a broad spectrum of industrial applications [1]. Adding $ZrO_2$ at different volume percentages (5, 10, and 15) enhances strength, corrosion resistance, and wear resistance. SEM analysis and wear testing reveal that 15% $ZrO_2$ addition to A390 alloy increases hardness and wear resistance, making it ideal for applications demanding exceptional durability [2]. Industries like aerospace and automotive require strong, lightweight materials. Metal Matrix Composites (MMCs) are highly promising because they can be customized to offer superior physical and mechanical properties tailored for specific applications [3]. The ultimate characteristics of a composite material are dictated by a combination of four key elements: the choice of the base alloy matrix, the nature of the reinforcing particles introduced, the specific manufacturing processes employed, and the intrinsic properties of those reinforcing materials themselves [4]. MMC that more reinforcing particles form thicker protective layers, reducing wear rate [5]. Hexagonal Boron Nitride (HBN) functions as a solid lubricant due to its lamellar structure and weak Vander Waals interactions [6]. Powder metallurgy for aluminium composite fabrication, overcoming slow cooling rates and achieving better particle dispersion for improved wear resistance [7]. The investigation of the wear characteristics in Al6061/$Al_2O_3$ composites produced by using in-situ powder metallurgy demonstrated that the incorporation of larger $Al_2O_3$ particles, with an average size of 150 m, resulted in a decrease in the wear rate of the composite material [8]. The impact of varying $TiB_2$ levels on Al7075, noting increased micro hardness with $TiB_2$ incorporation. Optimal wear resistance was observed with over 15% reinforcement, while higher TiB2 proportions and sliding distances correlated with elevated wear rates [9]. In a study of powder metallurgy, research revealed that increasing the iron (Fe) content improved both the hardness and strength of the resulting material; however, this enhancement came at the cost of reduced friction coefficient stability and a subsequent increase in wear rates. The material demonstrated optimal properties when the composition was precisely controlled at 14% Fe and 20% graphite [10]. Adding graphene oxide (GO) to composites made with the CoCrFeNiMn high-entropy alloy dramatically boosts their wear resistance. This combination increased the material's microhardness by 66.7% and lowered the overall wear rate by 78.3%. The improved performance is due to the even spread of tough chromium carbide ($Cr_7C_3$) particles throughout the material and a strong bond between these particles and the alloy, making the composite much tougher against scratches and better suited for demanding engineering uses [11]. Forming limit diagrams of aluminum-copper composites through powder metallurgy, examining density variations and copper content. Compression trials evaluated material properties, while densification curves analyzed pore closure during deformation [12]. Investigate coarse tungsten carbide with 10% and 12% cobalt sintered microstructures, suitable for Binder Jetting 3D printing. These materials exhibit mechanical properties and wear resistance comparable to commercially manufactured carbides, enabling effective printing of components with diverse sizes and intricate geometries [13]. Sintered $Al/Al_2O_3$ hybrid composites from aluminum dross waste, varying sintering temperatures and including graphene and SiC up to 4% and 8% wt, respectively. Enhanced properties observed with increased sintering temperature and reinforcement content [14]. CoCrFeMnNiHEA composites with $HfO_2$ nanoparticles, noting improved mechanical properties with increased $HfO_2$ levels, recommending them for advanced structural applications [15]. The tribological behavior of AA6061 composites with stir-cast zinc oxide (ZnO) particles. Chemical analysis via X-ray photoelectron spectroscopy and density measurements was conducted. Pin-on-disc tribometers assessed dry sliding wear under various stresses. Results showed uniform distribution of ZnO particles in the Al matrix, enhancing Vickers hardness values in the ZnO-reinforced samples [16]. Decreased wear rate and friction coefficient in MMCs due to improved bonding, reducing plastic deformation. Aluminium composites fabricated via vortex process and die casting, exhibited superior performance, offering cost-effective near-net shape production and promising advancements in automotive and other industries [17].

This study explores Al-$Cr_3C_2$ composites using optimized carbide dispersion to enhance high-temperature strength and wear resistance. Unlike SiC or$Al_2O_3$ reinforcements, $Cr_3C_2$ offers superior toughness and oxidation stability. The novelty lies in adjusting $Cr_3C_2$ content and processing conditions to achieve improved mechanical and tribological properties.

Previous research on Al composites mainly focuses on SiC, $Al_2O_3$, and TiC, with limited studies on $Cr_3C_2$ reinforcement. The influence of $Cr_3C_2$ on high-temperature wear, interfacial bonding, and microstructural stability is not well investigated. There is also a lack of systematic comparison of different $Cr_3C_2$ percentages and their combined effects on composite performance.

## 2. EXPERIMENTAL PROCEDURE

### 2.1 Materials

$Cr_3C_2$ and aluminium were chosen for their wear and corrosion resistance, respectively. The powders, bought from SRL lab and Parishwamani Metals, Mumbai, were 99.9% pure $Cr_3C_2$ and aluminium were selected for their wear and corrosion resistance. The powders from SRL Lab and Parishwamani Metals, Mumbai, were 99.9% pure with a 10 μm particle size. High purity was ensured to avoid contamination, as confirmed by supplier certificates. The particle size is 10 μm. $Cr_3C_2$ was selected for its limited solubility with aluminium, preventing the formation of hard phases and preserving ductility despite strength loss.

### 2.2 Methodology

$Al/Cr_3C_2$ composites were produced via powder metallurgy, following a procedure detailed in the studies [18, 19]. Four sample types with varying volume fractions of matrix and reinforcing materials were generated. Chromium carbide volume percentage was chosen based on literature. Powders were weighed and combined using a planetary ball mill, then compressed into green compacts and sintered at 530℃ for 90 minutes.

Porosity was estimated using the equation:

$$\text{Porosity} = (\text{Theoritical density} - \text{Experimental density}) / (\text{Theoritical density}) \times 100 \quad (1)$$

Dry sliding wear experiments were performed on polished and cleaned cylindrical pins, which slide against an EN 31 steel disc. $Cr_3C_2$ content, applied load, and sliding distance were investigated in this study.

Volume loss was calculated using the formula:

$$V=\pi R2(L1-L2) \quad (2)$$

where, V = volume loss, R = pin radius, L1 = pin length before testing, and L2 = pin length after testing.

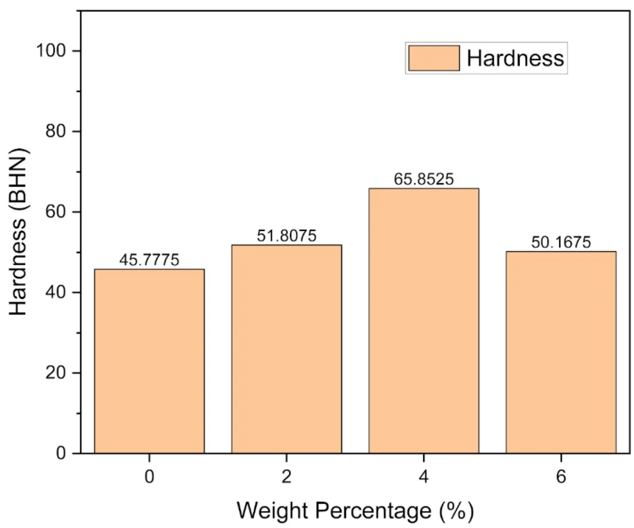


**Figure 1.** Influence of $Cr_3C_2$ reinforcement on hardness of aluminium composites

### 2.3 Micro hardness

Vickers hardness test was conducted to determine the optimal abrasion resistance for both MMC and base metal samples. Initially samples are cleaned with emery sheets and applied a 20-second load to assess performance. Optimizing surface flatness improved the holding mechanism and weight distribution.

**Table 1.** Results of hardness

| S.NO | Composition | Micro Hardness (VHC) |
|---|---|---|
| 1 | Al | 45.77 |
| 2 | Al-2%$Cr_3C_2$ | 51.80 |
| 3 | Al-4%$Cr_3C_2$ | 65.85 |
| 4 | Al-6%$Cr_3C_2$ | 50.16 |

Figure 1 depicts how the hardness of aluminium changes with different weight percentages of $Cr_3C_2$ reinforcement. As listed in Table 1. Incorporating 2 wt% $Cr_3C_2$ into the aluminium matrix alloy notably increased hardness by 13.17%. As the concentration of $Cr_3C_2$ reinforcement increases, so does the hardness of the aluminium matrix alloy.

The increase in $Cr_3C_2$ content from 2% to 4% resulted in a 43.87% improvement in hardness. Nevertheless, the introduction of a higher concentration (6 wt%) of $Cr_3C_2$ reinforcement inside the base matrix results in a reduction of hardness to 9.59%. The non-uniform distribution of reinforcing particles within the aluminum alloy might explain the observed decrease in hardness.

### 2.4 Wear testing of composite

To assess the dry sliding wear of composite specimens, the pin-on-disc test system was used. Metallographic pins with a diameter of 10 mm and length of 30 mm were manufactured, cut, and polished. After cleaning with acetone and drying, all samples were weighed to an accuracy of 0.0001 g on a single-pan electronic balance. Figure 2 illustrates the pin-on-disc apparatus employed for investigating wear phenomena. A load was applied to the pin to maintain equilibrium against a hardened EN32 steel disc (67 HRC). All specimens exhibited circular motion with a 110 mm diameter under tangential force. Wear detection was enabled by a load cell (LVDT) on the lever arm, transmitting signals to the computer. The coefficient of friction was measured from the combined data. Following each test, specimens were cleansed with acetone. The specimens were reweighed to estimate the volumetric wear rate. This rate was calculated by converting mass loss to volume loss and dividing by sliding distance.

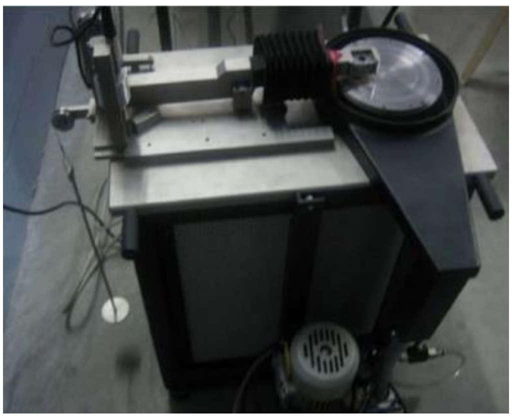

**Figure 2.** Pin-on-disc machine

The parameters for the wear test are outlined as follows:

- The weight proportions of $Cr_3C_2$ at concentrations of 0%, 2%, 4%, and 6% are being considered.
- The load was applied at four different magnitudes: 15 N, 30 N, 45 N, and 60 N.
- The sliding velocities considered in this study are 1 m/s, 1.5 m/s, and 2 m/s.
- The distances covered during the sliding activity were 500, 1000, 1500, and 2000 meters.

## 3. RESULTS AND DISCUSSIONS

### 3.1 Wear behaviour of MMCS

This work explores the dry sliding wear properties of Al/$Cr_3C_2$ composites, with a focus on how applied load, reinforcement ratio, and sliding speed affect wear. The impact of varying sliding speeds and the presence of reinforcement materials on the rate of wear is examined in Section 3.2.

### 3.2 Influence of sliding speed and reinforcement on wear resistance of Al/$Cr_3C_2$ composites

Applied load increases the real contact area and intensifies plastic deformation; $Cr_3C_2$ particles counter this by bearing the load, but excessive load can cause particle debonding and shift the wear regime to severe. Sliding speed mainly affects frictional heating: higher speeds soften the matrix and promote adhesive wear unless a stable, oxide-rich tribolayer forms, which the $Cr_3C_2$ reinforcement helps to strengthen.

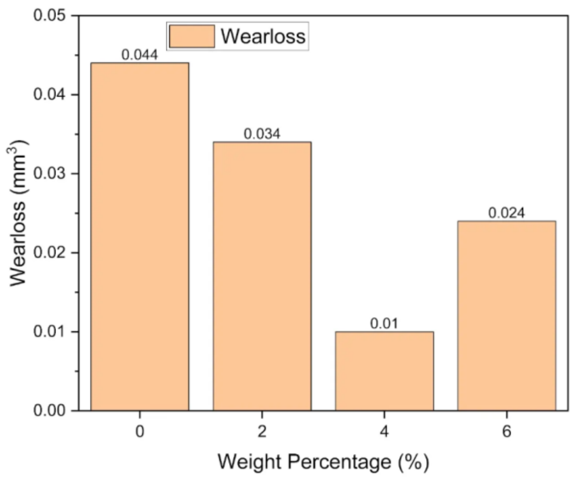


**Figure 3.** Investigating the impact of a sliding speed 1 m/s on the wear rate of composites reinforcements by weight

Figures 3-5 depict how sliding velocity affects the wear rate for composites with weight reinforcements of 15, 30, 45, and 60 N, while maintaining a constant sliding distance of 2000 m. The graphs show a decline in the wear rate of composites until reaching an approximate velocity of 2 meters per second. The decrease in wear rate is ascribed to the formation of an oxide layer resulting from the oxidation of the aluminium alloy at high interfacial temperatures. Iron oxide coatings formed during wear exhibit solid lubricating properties, leading to reduced wear rates. oxidation occurred in iron due to wear. Unreinforced alloys exhibit higher wear rates compared to composites under various loading conditions [20]. Incorporating $Cr_3C_2$ into pure aluminium improves its wear resistance under dry sliding conditions. Wear rate is directly proportional to sliding velocity, with minimized wear at a sliding speed of 1 m/s and a 4% weight content of chromium carbide ($Cr_3C_2$). A reduction in wear with increased sliding velocity for the aluminium chromium carbide composite due to oxidation of aluminium particles at the contact surface interface [21].

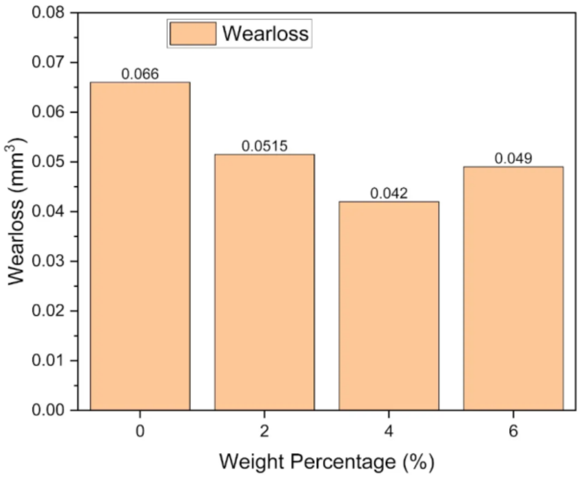


**Figure 4.** Investigating the effect of a sliding speed 1.5 m/s on the wear rate of composites reinforcements by weight

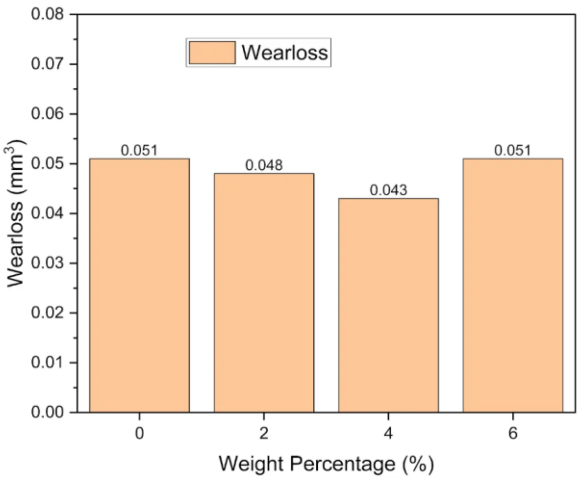


**Figure 5.** Investigating the effect of a sliding speed 2 m/s on the wear rate of composites reinforcements by weight

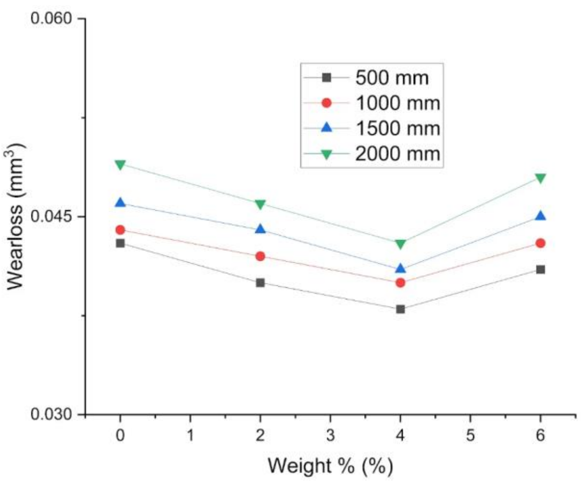


**Figure 6.** Weight% & sliding distance vs. wear loss at 2 m/s

The study investigates wear loss at velocities of 1, 1.5, and 2 m/s, considering different $Cr_3C_2$ reinforcement percentages. Due to minimal wear fluctuation in Figures 3-5, focus shifts to 2 m/s velocity (Figure 6).

Wear decreases by 5.8% and 10% with a 0% to 4% reinforcement increase. Additional mass leads to an 18% rise in wear. Findings suggest consistent low wear loss, at 4% by weight, regardless of velocity. However, at 4% reinforcement, wear is lowest at a sliding distance of 500mm, increasing with distance.

Figure 7 depicts wear loss variance with distance across different reinforcement percentages. Wear is minimal at shorter sliding distances but increases progressively with longer distances. Regardless of sliding extent, wear loss decreases with up to 4% chromium carbide content, then rises. Initially, higher wear rates result from smooth chromium carbide surfaces lacking roughness projections, causing uniform stress distribution and subsequent wear. As reinforcement proportion increases, friction force rises, leading to increased disengagement and specimen fracture, escalating wear loss.

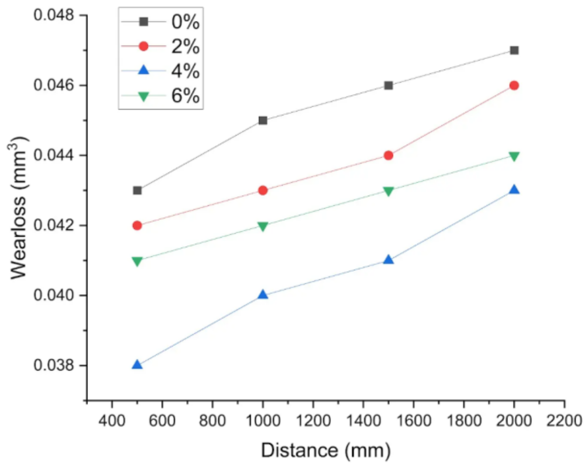


**Figure 7.** Distance vs. wear loss at 2 m/s

### 3.3 Effect of load and reinforcement on wear rate

Figure 8 depicts the correlation between wear loss and the weight percentage of reinforcement at various loads. Research has demonstrated that the wear loss of metal-matrix composites follows a decreasing trend with an increase in chromium carbide content, irrespective of the applied load. This trend continues until a specific threshold (4%) is reached. However, above this threshold, the wear loss starts to increase with an increase in $Cr_3C_2$% concentration. At higher magnitudes of applied force, the frictional resistance experiences an augmentation as a result of the escalating pressure exerted on the contact surface. This leads to the accumulation of heat at the interface, consequently resulting in a greater degree of wear. Above 4% reinforcement, high loads generate excessive heat and plastic deformation in the aluminium matrix, weakening the particle-matrix bond. This causes $Cr_3C_2$ particles to detach and act as abrasive third bodies, increasing micro-cutting and wear. Under such conditions, the high-load thermal and mechanical stresses outweigh the benefits of added reinforcement, leading to higher wear even at greater than 4% $Cr_3C_2$.

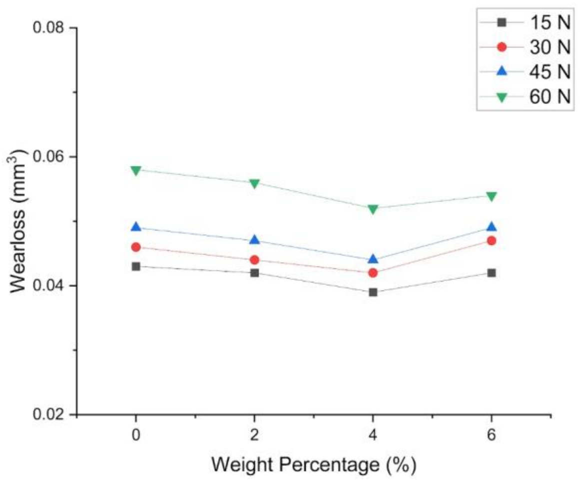


**Figure 8.** Wear loss varying wt%

### 3.4 Temperature rise and wear mechanisms in sliding contacts

The investigation on HMMC thermal behavior explores temperature fluctuations. A thermocouple inserted into perforated samples measures temperature disparity pre and post-process. Figures 9-11 show a direct link between applied load and temperature rise in worn samples. Frictional heat generation during wear elevates sample temperature, notably at contact points. This increase heightens wear and friction, more pronounced in monolithic alloys than MMCs. Al/4% $Cr_3C_2$ composites exhibit the lowest temperature rise, enhancing aluminum's thermal stability. Regardless of sliding speed, this pattern persists. The temperature increase in MMCs aligns with wear rate responses under pressure, indicating superior attrition resistance in Al/4% $Cr_3C_2$ composite compared to others.

Rising temperature softens aluminium, making it more prone to deformation and wear, while also accelerating oxidation and destabilizing the tribolayer. In MMCs, $Cr_3C_2$ particles resist softening and help maintain a stable protective layer, reducing heat buildup. As a result, Al/$Cr_3C_2$ composites show much better high-temperature wear performance than monolithic aluminium.

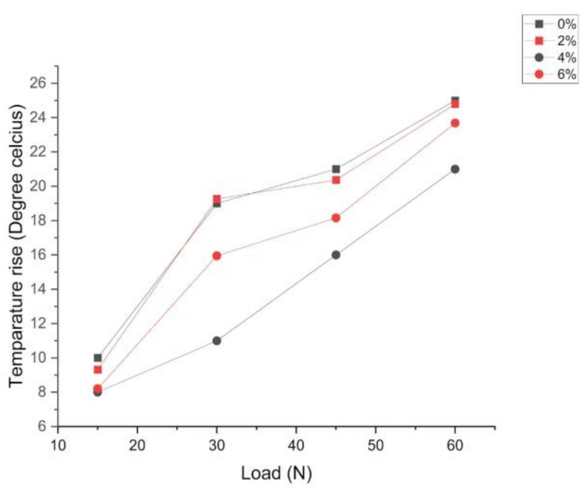


**Figure 9.** Temperature elevation of composites under applied loads at a sliding speed of 1 m/s

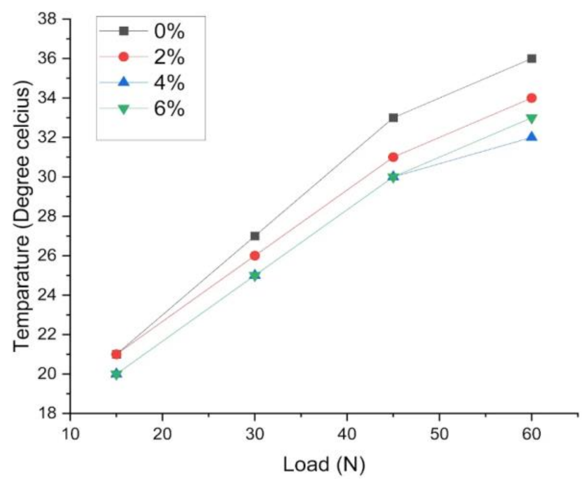


**Figure 10.** Temperature elevation of composites under applied loads at a sliding speed of 1.5 m/s

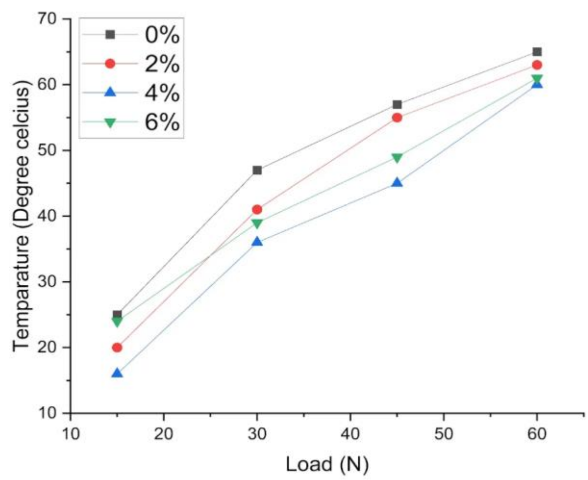


**Figure 11.** Temperature elevation of composites under applied loads at a sliding speed of 2 m/s

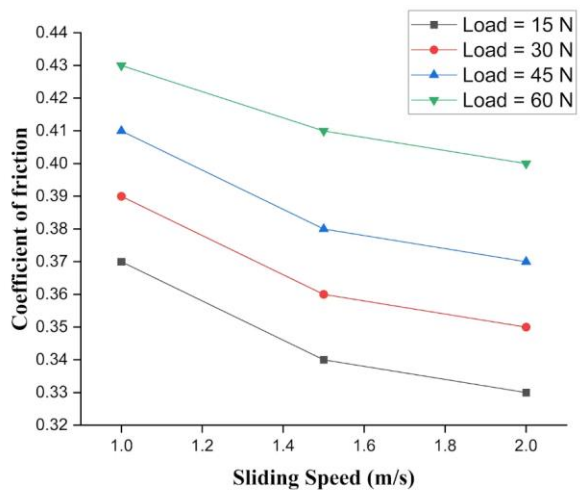


**Figure 12.** Variation of sliding speed with coefficient of friction Al/2% $Cr_3C_2$

### 3.5 Coefficient of friction measurement

The coefficient of friction quantifies how much resistance there is to sliding between two surfaces in contact. Frictional forces act perpendicular to any motion between the surfaces and are expressed as a percentage of the reaction force. This coefficient varies linearly with both the applied load and the velocity of sliding. Figures 12-14 illustrate how the coefficient of friction changes with sliding velocity. Notably, both composite materials and solid alloys show a significant decrease in friction with higher sliding speeds, irrespective of the applied load. The inclusion of graphite particles, known for their natural lubricating properties, further reduces frictional heat generation. Additionally, increasing the $Cr_3C_2$ content also lowers friction [22]. At low sliding speeds, friction remains constant regardless of surface velocity, but as speed increases, the coefficient of friction decreases.

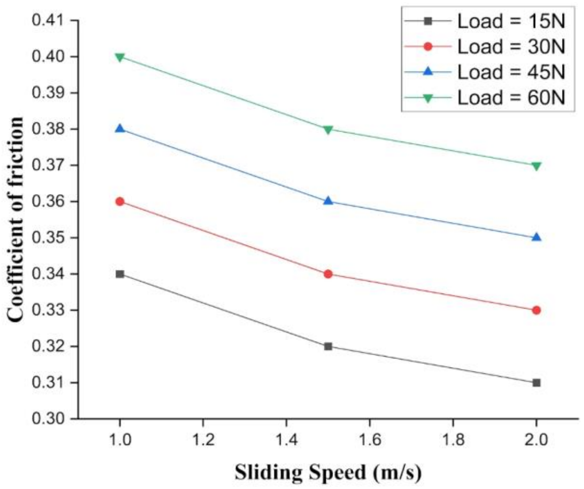


**Figure 13.** Variation of sliding speed with coefficient of friction Al/4% $Cr_3C_2$

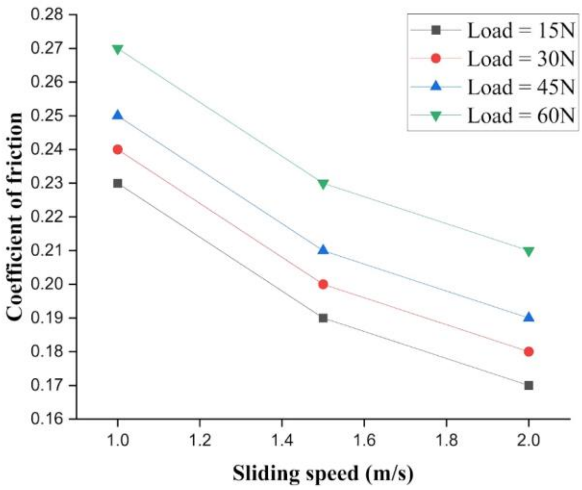


**Figure 14.** Variation of frictional coefficient with sliding speed for Al/6% $Cr_3C_2$

## 4. SEM INVESTIGATIONS OF WEAR SPECIMEN

SEM analysis was employed to study the worn surfaces of aluminium and its composites, aiming to gain insight into the wear mechanism. While sliding, the entire surface of the pin interfaces with the steel disc, unveiling machine markings present on the disc. Micrographs (Figures 15-18) display the worn surface of aluminium alloys and composites under specific conditions: 40 N applied stress, 2 m/s sliding speed, and 2000 mm sliding distance, across various weight percentages of $Cr_3C_2$. The micrograph of the aluminium alloy indicates greater material depletion from the surface of the pin during wear. Increasing the $Cr_3C_2$ reinforcement content results in a reduction in both the depth and quantity of surface grooves on the pin, thereby enhancing fatigue resistance. Additionally, MMCs demonstrate lower friction and wear rates in comparison to matrix alloys, attributed to the inclusion of graphite particles [23].

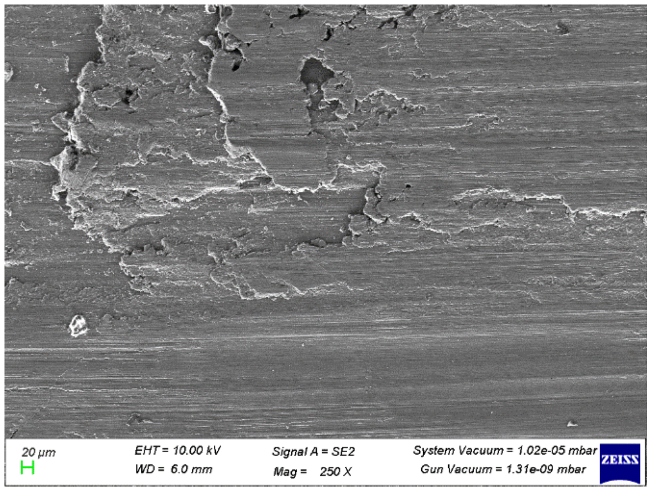


**Figure 15.** SEM image of 0% $Cr_3C_2$

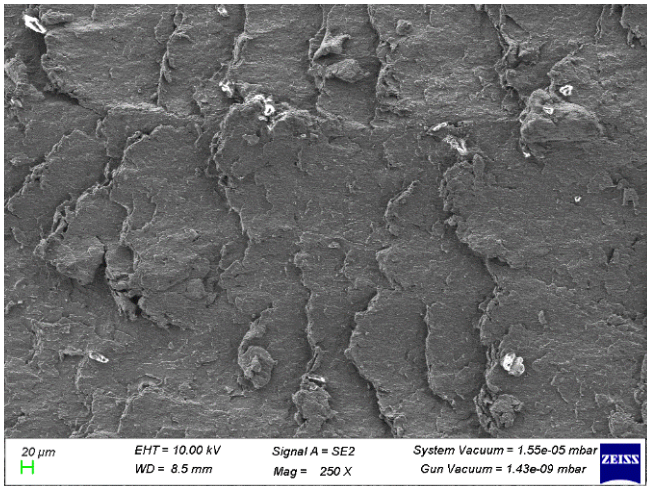


**Figure 16.** SEM image of 2% $Cr_3C_2$

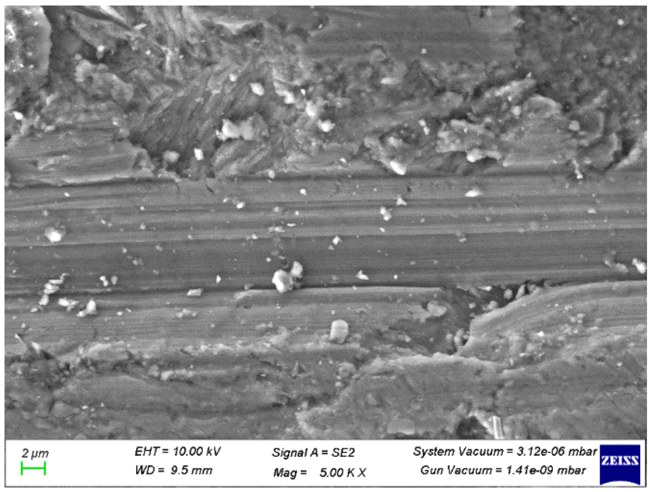


**Figure 17.** SEM image of 4% $Cr_3C_2$

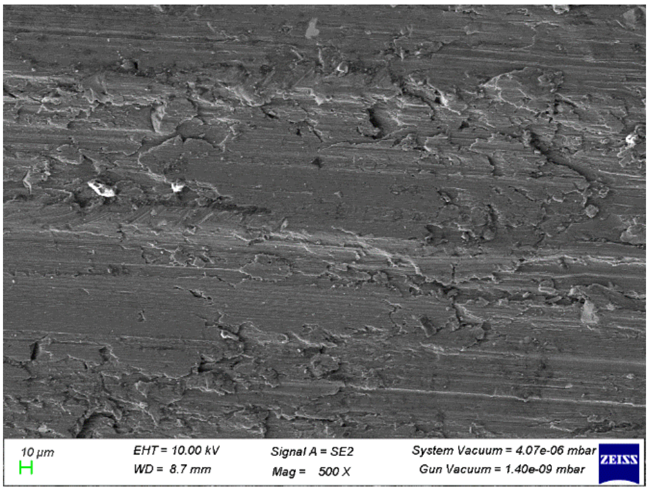


**Figure 18.** SEM image of 6% $Cr_3C_2$

For more comprehensive validation of the observed wear mechanisms, future work should include EDS/EDX analysis to confirm the elemental composition of wear debris, oxide layers, and embedded $Cr_3C_2$ particles. Such chemical mapping would help distinguish oxide formation from metallic wear tracks and verify the distribution or pull-out of reinforcement particles. If available, integrating EDS results would strengthen the interpretation of tribological behaviour in Al/ $Cr_3C_2$ composites.

## 5. CONCLUSIONS

The mechanical properties of MMC as well as the material's dry sliding wear behaviour have been examined.

•The toughness of MMCs has significantly improved. For composites containing 4 wt% $Cr_3C_2$, uniform reinforcement distribution was accomplished with strong matrix-reinforcement bonding.

•Incorporating $Cr_3C_2$ particles enhances the toughness of the resulting composites. Research reveals that composites reinforced with 4 wt% $Cr_3C_2$ exhibit the highest hardness, measuring at 65.54 BHN.

•Regardless of $Cr_3C_2$ composition, the wear loss of prepared composites increased with increasing applied load. Composites have the lowest volume loss at 4 wt% when compared to others. The Al/4 wt% $Cr_3C_2$ composite is a promising material for usage in gears, drive shafts, brake drums, and bearings.

•This statement contrasts with the typical trend of wear rate and coefficient of friction decreasing as sliding speed increases.

•Regardless of the environment in which they are utilised, the wear rate of MMCs is consistently lower than that of Al. The Al/4 wt% $Cr_3C_2$ composite exhibits the maximum wear resistance when compared to an Al. As the proportion of reinforcement in the alloy increases, the rate of wear reduces. During the wearing process, temperature rise is also detected, and it was determined that the temperature rise of the wear sample increases as load increases. The observation that the temperature rise of the worn sample increases with load led to this discovery. The level of damage was greater in alloys than in composites, and the depth and number of grooves increased with increasing sliding speed and load, according to SEM analysis of the worn surfaces of the specimens.

The Al/4 wt% $Cr_3C_2$ composite delivers the best toughness, hardness, and wear resistance with excellent thermal stability, making it ideal for high-load applications such as gears, drive shafts, brake drums, and bearings.

## ACKNOWLEDGMENT

The authors acknowledge the Sophisticated Analytical Instruments Facility, DST-India for providing SEM facilities.

## REFERENCES

[1] Dolata, A. J., Dyzia, M., Wieczorek, J. (2019). Tribological properties of single (AlSi7/SiCp, AlSi7/GCsf) and hybrid (AlSi7/SiCp + GCsf) composite layers formed in sleeves via centrifugal casting. Materials, 12(17): 2803. https://doi.org/10.3390/ma12172803

[2] Karthikeyan, S., Karunanithi, R., Ghosh, A. (2020). Investigation on microstructures, mechanical and wear properties of Al 390/$ZrO_2$ composite materials fabricated by P/M method. Multidiscipline Modeling in Materials and Structures, 17(1): 149-166. https://doi.org/10.1108/mmms-10-2019-0180

[3] Rimal, A., Natarajan, V. D. (2024). Comparative analysis of aerodynamic and structural performance of aircraft wings using boron aluminum metal matrix composites and aluminum alloys: A CFD and FSI approach. Precision Mechanics & Digital Fabrication, 1(2): 75-90. https://doi.org/10.56578/pmdf010203

[4] Dasgupta, R. (2012). Aluminium alloy-based metal matrix composites: A potential material for wear resistant applications. International Scholarly Research Notices, 2012(1): 594573. https://doi.org/10.5402/2012/594573

[5] Wasekar, N.P., Bathini, L., Ramakrishna, L., Rao, D.S., Padmanabham, G. (2020). Pulsed electrodeposition, mechanical properties and wear mechanism in Ni-W/SiC nanocomposite coatings used for automotive applications. Applied Surface Science, 527: 146896. https://doi.org/10.1016/j.apsusc.2020.146896

[6] Mahathanabodee, S., Palathai, T., Raadnui, S., Tongsri, R., Sombatsompop, N. (2014). Dry sliding wear behavior of SS316L composites containing h-BN and $MoS_2$ solid lubricants. Wear, 316(1-2): 37-48. https://doi.org/10.1016/j.wear.2014.04.015

[7] Wang, H.S., Chen, H.G., Gu, J.W., Hsu, C.E., Wu, C.Y. (2014). Effects of heat treatment processes on the microstructures and properties of powder metallurgy produced Cu-Ni-Si-Cr alloy. Materials Science and Engineering: A, 619: 221-227. https://doi.org/10.1016/j.msea.2014.09.098

[8] Pournaderi, S., Akhlaghi, F. (2017). Wear behaviour of Al6061-$Al_2O_3$ composites produced by in-situ powder metallurgy (IPM). Powder Technology, 313: 184-190. https://doi.org/10.1016/j.powtec.2017.03.019

[9] Loganathan, P., Gnanavelbabu, A., Rajkumar, K. (2021). Effect of $TiB_2$ particles on high temperature wear and friction behaviour of AA7075 composites fabricated through squeeze cast technique. Materials Today: Proceedings, 45: 7859-7864. https://doi.org/10.1016/j.matpr.2020.12.430

[10] Prabhu Deva, M., Parthiban, A., Radha Krishnan, B.,

Haile, A., Degife, W. (2022). Investigation of wear behaviour and mechanical properties of titanium diboride reinforced AMMC composites. Advances in Materials Science and Engineering, 2022(1): 5144010. https://doi.org/10.1155/2022/5144010

[11] Zheng, D., Zhao, X., An, K., Chen, L., Zhao, Y., Khan, D. F., Qu, X., Yin, H. (2023). Effects of Fe and graphite on friction and wear properties of brake friction materials for high-speed and heavy-duty vehicles. Tribology International, 178: 108061. https://doi.org/10.1016/j.triboint.2022.108061

[12] Ye, W., Xie, M., Huang, Z., Wang, H., Zhou, Q., Wang, L., Chen, B., Wang, H., Liu, W. (2023). Microstructure and tribological properties of in-situ carbide/CoCrFeNiMn high entropy alloy composites synthesized by flake powder metallurgy. Tribology International, 181: 108295. https://doi.org/10.1016/j.triboint.2023.108295

[13] Wolla, D.W., Davidson, M.J., Khanra, A.K. (2014). Studies on the formability of powder metallurgical aluminum–copper composite. Materials & Design, 59: 151-159. https://doi.org/10.1016/j.matdes.2014.02.049

[14] Wolfe, T., Shah, R., Prough, K., Trasorras, J.L. (2023). Coarse cemented carbide produced via binder jetting 3D printing. International Journal of Refractory Metals and Hard Materials, 110, 106016. https://doi.org/10.1016/j.ijrmhm.2022.106016

[15] Taha, M.A., Zawrah, M.F., Abomostafa, H.M. (2022). Fabrication of Al/$Al_2O_3$/ SiC/graphene hybrid nanocomposites from Al-dross by powder metallurgy: Sinterability, mechanical and electrical properties. Ceramics International, 48(14): 20923-20932. https://doi.org/10.1016/j.ceramint.2022.04.084

[16] Nagarjuna, C., Sharma, A., Lee, K., Hong, S.J., Ahn, B. (2023). Microstructure, mechanical and tribological properties of oxide dispersion strengthened CoCrFeMnNi high-entropy alloys fabricated by powder metallurgy. Journal of Materials Research and Technology, 22: 1708-1722. https://doi.org/10.1016/j.jmrt.2022.12.070

[17] RM, S.S., K, R., BV, B., R, R. (2021). A study on tribological behaviour and analysis of ZnO reinforced AA6061 matrix composites fabricated by stir casting route. Industrial Lubrication and Tribology, 73(4): 642-651. https://doi.org/10.1108/ILT-11-2020-0392

[18] Kathiresan, M., Sornakumar, T. (2010). Friction and wear studies of die cast aluminum alloy-aluminum oxide-reinforced composites. Industrial Lubrication and Tribology, 62(6): 361-371. https://doi.org/10.1108/00368791011076263

[19] Kumar, N., Bharti, A., Saxena, K.K. (2021). A re-investigation: Effect of powder metallurgy parameters on the physical and mechanical properties of aluminium matrix composites. Materials Today: Proceedings, 44: 2188-2193. https://doi.org/10.1016/j.matpr.2020.12.351

[20] Kumar, N., Bharti, A., Dixit, M., Nigam, A. (2020). Effect of powder metallurgy process and its parameters on the mechanical and electrical properties of copper-based materials: Literature review. Powder Metallurgy and Metal Ceramics, 59(7-8): 401-410. https://doi.org/10.1007/s11106-020-00174-1

[21] Alpas, A.T., Zhang, J. (1992). Effect of SiC particulate reinforcement on the dry sliding wear of aluminium-silicon alloys (A356). Wear, 155(1): 83-104. https://doi.org/10.1016/0043-1648(92)90111-K

[22] Basavarajappa, S., Chandramohan, G., Mukund, K., Ashwin, M., Prabu, M. (2006). Dry sliding wear behavior of Al 2219/SiCp-Gr hybrid metal matrix composites. Journal of Materials Engineering and Performance, 15(6): 668-674. https://doi.org/10.1361/105994906x150803

[23] Deuis, R.L., Subramanian, C., Yellup, J.M. (1997). Dry sliding wear of aluminium composites—A review. Composites Science and Technology, 57(4): 415-435. https://doi.org/10.1016/S0266-3538(96)00167-4